

Coulomb blockade and Non-Fermi-liquid behavior in quantum dots

Frithjof B. Anders,¹ Eran Lebanon,² and Avraham Schiller²

¹*Department of Physics, Universität Bremen, P.O. Box 330 440, D-28334 Bremen, Germany*

²*Racah Institute of Physics, The Hebrew University, Jerusalem 91904, Israel*

The non-Fermi-liquid properties of an ultrasmall quantum dot coupled to a lead and to a quantum box are investigated using a new variant of Wilson's numerical renormalization group. Below the charging energy of the quantum box, a second screening channel is dynamically generated. Tuning the ratio of the tunneling amplitudes to the lead and box, we find a two-channel Kondo fixed point for arbitrary Coulomb repulsion on the dot. For an asymmetric dot, we find a continuous transition from a spin to a charge two-channel Kondo effect. At $T = 0$, a step-like structure is found in the conductance of a two-lead setting, the height of which depends on the dot occupancy. The temperature scale below which the two-channel Kondo effect sets in is greatly enhanced away from the local-moment regime, making this exotic effect accessible in realistic quantum-dot devices.

PACS numbers: 73.23.Hk, 72.15.Qm, 73.40.Gk

Recently, Oreg and Goldhaber-Gordon (OGG) [1] proposed a new realization of the two-channel Kondo effect (2CKE) in quantum-dot systems. These authors cleverly noticed that the inter-lead exchange coupling, which spoils the two-channel Kondo picture for an ultrasmall dot in a two-lead setting, can be switched off if one of the leads is replaced by a quantum box (i.e., a large dot). This stems from the suppression of charge fluctuations on the quantum box, for temperatures well below its charging energy. To this end, the quantum box has to be tuned to a Coulomb-blockade valley. A spin 2CKE then develops on the ultrasmall dot if the effective spin-exchange couplings to the lead and box are tuned to be equal.

The scenario of OGG assumes the formation of a stable local moment on the ultrasmall dot. Here we show that the occurrence of a spin 2CKE is far more generic to the lead-dot-box setting, extending to the mixed-valent regime of the ultrasmall dot, and away from the Coulomb-blockade valley of the quantum box. In fact, one can tune the system to a spin 2CKE even for a non-interacting dot, which we explain by the approach to perfect transmission through the dot. Away from particle-hole symmetry we find an intriguing entanglement of spin and charge degrees of freedom within the 2CKE that develops, reflected in the simultaneous log-divergence of the magnetic susceptibility of the dot and the charge capacitance of the box. Indeed, the spin 2CKE of OGG is continuously connected to a charge 2CKE of the type proposed by Matveev [2]. A step-like structure is found in the $T = 0$ conductance of a two-lead device, the height and shape of which depends on the dot occupancy.

The setting we consider consists of an ultrasmall quantum dot, modeled by a single energy level ϵ_d and an on-site repulsion U , embedded between a metallic lead and a quantum box. The quantum box is characterized by a finite charging energy, E_C , and by a dense set of single-particle levels, which we take to be continuous. Denoting the creation of an electron with spin projection σ on the

dot by d_σ^\dagger , the corresponding Hamiltonian reads

$$\mathcal{H} = \sum_{\alpha=L,B} \sum_{k,\sigma} \epsilon_{\alpha k} c_{\alpha k \sigma}^\dagger c_{\alpha k \sigma} + E_C (\hat{n}_B - N_B)^2 \quad (1)$$

$$+ \epsilon_d \sum_{\sigma} d_\sigma^\dagger d_\sigma + U \hat{n}_{d\uparrow} \hat{n}_{d\downarrow} + \sum_{\alpha,k,\sigma} t_\alpha \left\{ c_{\alpha k \sigma}^\dagger d_\sigma + \text{H.c.} \right\},$$

where $c_{Lk\sigma}^\dagger$ ($c_{Bk\sigma}^\dagger$) creates a lead (box) electron with momentum k and spin projection σ , t_L (t_B) is the tunneling matrix element between the quantum dot and the lead (box), ϵ_{Lk} (ϵ_{Bk}) are the single-particle levels in the lead (box), and $\hat{n}_{d\sigma} = d_\sigma^\dagger d_\sigma$ are the number operators on the dot. The excess number of electrons inside the box, $\hat{n}_B = \sum_{k\sigma} [c_{Bk\sigma}^\dagger c_{Bk\sigma} - \theta(-\epsilon_{Bk})]$, is controlled by the dimensionless gate voltage, N_B .

We treat the Hamiltonian of Eq. (1) using Wilson's numerical renormalization-group method (NRG) [3]. The main complication in applying the NRG to the Hamiltonian of Eq. (1) stems from the charging energy of the box electrons. To this end, we employ a recent adaptation of the NRG to the Coulomb blockade [4], based on a mapping due to Schoeller and co-workers [5]. Introducing three new collective charge operators for the box,

$$\hat{N} = \sum_{m=-\infty}^{\infty} m |m\rangle\langle m| \quad \text{and} \quad \hat{N}^\pm = \sum_{m=-\infty}^{\infty} |m\pm 1\rangle\langle m|, \quad (2)$$

we replace the tunneling term between the dot and the box in Eq. (1) with $\sum_{k,\sigma} t_B \left\{ \hat{N}^+ c_{Bk\sigma}^\dagger d_\sigma + \text{H.c.} \right\}$, while the charging-energy term is converted to $E_C (\hat{N} - N)^2$. This yields an exact mapping of the Hamiltonian of Eq. (1), provided the constraint $\hat{N} = \hat{n}_B$ is enforced. In the continuum limit, one can conveniently relax this constraint, as the dynamics of \hat{N} within the resulting Hamiltonian is insensitive to the precise number of conduction electrons in the bands. Hence, \hat{N} can be treated as an independent degree of freedom.

At the conclusion of these steps, one is left with a Hamiltonian describing two noninteracting conduction

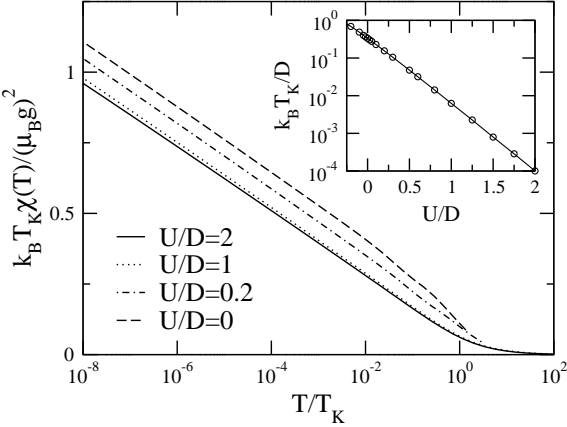


FIG. 1: The magnetic susceptibility of the dot versus T , for $\Gamma_L = E_C = 0.1D$, $N_B = 0$, and different values of $U = -2\epsilon_d$. Here Γ_B is tuned for each value of U to the two-channel point $\Gamma_B^{2\text{CK}}$. T_K is the Kondo temperature defined in Eq. (3). For all U , ranging from the local-moment regime $U \gg \Gamma_L$, to the strongly mixed-valent regime $U = 0$, to negative U (not shown), there exists a two-channel point $\Gamma_B^{2\text{CK}}$ where $\chi(T)$ diverges logarithmically as $T \rightarrow 0$, and the finite-size spectrum converges to the conventional two-channel fixed point. Inset: T_K versus U . For $U \gg \Gamma_L, E_C$ (local-moment regime), T_K decreases approximately exponentially with U . For $U < \Gamma_L$ (mixed-valent regime), it exceeds E_C .

bands coupled to a complex impurity, which we solve using the NRG. The fictitious impurity is composed of both \hat{N} and the dot degrees of freedom, and contains an infinite number of levels. In practice, only a finite subset of the \hat{N} states are kept, up to a high-energy cutoff ω_c several times larger than the bandwidth D (we use $\omega_c \geq 4D$). Box states whose charging energy exceeds ω_c contribute only insignificantly to the thermodynamics, and can be safely omitted. The number N_s of the NRG states retained sets a lower bound on the ratio E_C/D one can treat. As for the lead and box, we take the two conduction baths to have a common rectangular density of states: $\rho(\epsilon) = \rho\theta(D - |\epsilon|)$. The NRG discretization parameter [3] Λ is set equal to 2.8, while $N_s = 2000$.

We begin with a symmetric dot, $U = -2\epsilon_d$, and with a box tuned to the middle of a Coulomb-blockade valley, $N_B = 0$. Fixing E_C and the hybridization strength to the lead, $\Gamma_L = \pi\rho t_L^2$, we varied the hybridization to the box, $\Gamma_B = \pi\rho t_B^2$, in search of a 2CKE. Our results for $E_C = \Gamma_L = 0.1D$ are summarized in Fig. 1. Quite surprisingly, we find a two-channel Kondo point $\Gamma_B^{2\text{CK}}$ for all values of U , ranging from the local-moment regime $U \gg \Gamma_L$, to the strongly mixed-valent regime $U \approx 0$, to the unrealistic regime of $U < 0$. The development of a 2CKE is reflected in a log-divergence of the dot susceptibility as $T \rightarrow 0$ [6], see Fig. 1, and in a finite-size spectrum that converges to the conventional two-channel fixed point (i.e., identical energies and quantum numbers).

The emergence of a 2CKE for $U \gg \Gamma_L$ is in accord

with the scenario of OGG. Indeed, the associated Kondo temperature decays approximately exponentially with U for $U \gg \Gamma_L, E_C$ (inset of Fig. 1), while the ratio $\Gamma_B^{2\text{CK}}/\Gamma_L$ approaches the asymptotic value $1 + 2E_C/U$ [1] (not shown). Here and throughout the paper we define the Kondo temperature T_K according to the Bethe ansatz expression for the slope of the $\log-T$ diverging term in the susceptibility of the two-channel Kondo model [7]:

$$\chi(T) \sim \frac{(\mu_B g)^2}{20k_B T_K} \ln(T_K/T). \quad (3)$$

We emphasize, however, that the NRG goes beyond the Schrieffer-Wolff transformation used in Ref. [1], confirming that no relevant perturbations are generated at higher orders in the tunneling amplitudes.

Contrary to the local-moment regime, the development of a 2CKE in the mixed-valent regime, let alone for a negative U , is a new feature, with no apparent spin degree of freedom to be overscreened. Moreover, T_K is significantly enhanced for $U \approx 0$, exceeding E_C in Fig. 1. This behavior is reminiscent of the two-channel Anderson model, where the 2CKE likewise persists into the mixed-valent regime [8]. Particularly intriguing is the limit of a noninteracting dot, which reduces to the well-studied problem of a quantum box connected to a lead by single-mode tunneling [9]. Although a charge 2CKE was predicted for the latter setting at the degeneracy points of the Coulomb blockade [2], no spin 2CKE was previously anticipated.

To understand the 2CKE for $U = 0$, we reconsider the problem of a quantum box connected to a lead by a nearly fully transmitting single-mode point contact. Following Flensberg [10] and Matveev [11], we model this system by a 1D geometry, where $x < 0$ ($x > 0$) represents the lead (box), and $x = 0$ corresponds to the noninteracting dot. Linearizing the electron dispersion about the Fermi points, we decompose the electron field into a left- and a right-moving part, $\psi_{L\sigma}(x)$ and $\psi_{R\sigma}(x)$. Hence \hat{n}_B is given by the excess occupancy of $\psi_{L\sigma}(x)$ and $\psi_{R\sigma}(x)$ for all $x > 0$ [10, 11]. The deviation from perfect transmission is modeled by weak back scattering at $x = 0$ [10, 11], while the local magnetic field acting on the dot is represented by $\mathcal{H}_{\text{mag}} = \frac{1}{2}\mu_B g H \sum_{\sigma} \sigma [\psi_{L\sigma}^{\dagger}(0)\psi_{R\sigma}(0) + \text{H.c.}]$. Here we retain only the back-scattering part of the local field, as it is responsible for any singular response.

Precisely this model was recently studied by Le Hur and Seelig using bosonization [12]. Extending their treatment to a finite temperature $k_B T \ll E_C$, and accounting for an underlying symmetry of the Hamiltonian [13], we obtain the following linear magnetic susceptibility:

$$\chi(T) = \chi_0 \left(\frac{\mu_B g}{\hbar v_F} \right)^2 \left[\ln \left(\frac{D_{\text{eff}}}{2\pi k_B T} \right) - \psi \left(\frac{1}{2} + \frac{\Gamma}{2\pi k_B T} \right) \right], \quad (4)$$

with $\chi_0 = \Gamma/(4\pi R)$ and

$$\Gamma = \frac{8\gamma E_C}{\pi^2} R \cos^2(\pi N_B). \quad (5)$$

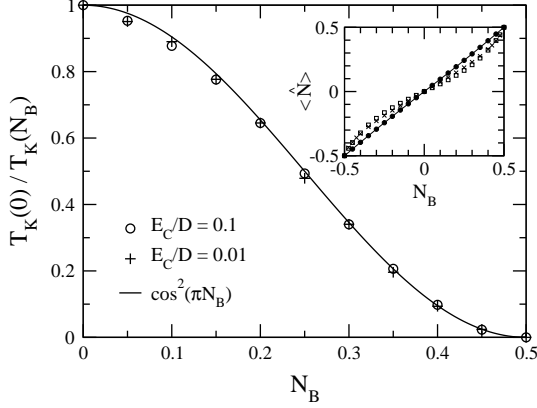


FIG. 2: $1/T_K$ versus N_B , for $U = \epsilon_d = 0$ and $\Gamma_L/D = 0.1$. Here E_C/D equals 0.1 (circles) and 0.01 (pluses). For each combined value of N_B and E_C , the coupling Γ_B is tuned to the two-channel point $\Gamma_B^{2\text{CK}}$. As a function of N_B , $\Gamma_B^{2\text{CK}}(N_B)$ varies by less than 0.2% for each fixed value of E_C . The ratio $T_K(0)/T_K(N_B)$ is well described by $\cos^2(\pi N_B)$ (solid line). Inset: The box charge $\langle \hat{N} \rangle$ versus N_B , for $\Gamma_L = E_C = 0.1D$ and $U = \epsilon_d = 0$. Here Γ_B/Γ_L equals 1 (squares), 1.72 (filled circles + solid line), and 3.24 (crosses). The Coulomb staircase is completely washed out for $\Gamma_B = \Gamma_B^{2\text{CK}}(0) = 1.72\Gamma_L$, but is gradually recovered upon departure from $\Gamma_B^{2\text{CK}}(0)$.

Here, R is the reflectance, v_F is the Fermi velocity, γ equals e^C with $C \approx 0.5772$, $\psi(x)$ is the digamma function, and D_{eff} is an effective cutoff of the order of E_C .

Equation (4) features a logarithmic temperature dependence down to $k_B T \sim \Gamma$. Hence, $\chi(T)$ diverges logarithmically for perfect transmission, when $\Gamma \propto R$ vanishes. In fact, $\chi(T)$ diverges logarithmically at perfect transmission for all gate voltages, except for half-integer values of N_B where χ_0 vanishes. In particular, Eqs. (4)–(5) predict $T_K(N_B) \propto 1/\cos^2(\pi N_B)$.

Equations (4)–(5) formally describe the limit $E_C \ll \Gamma_L$, since Γ_L serves as the effective bandwidth for the 1D model used [9]. Surprisingly, we find good agreement with the NRG results for $U = 0$ even for E_C as large as Γ_L : (i) Scanning N_B for fixed E_C and Γ_L , we find a 2CKE for all gate voltages, with a Kondo temperature that varies as $T_K(N_B) \propto 1/\cos^2(\pi N_B)$ (Fig. 2); (ii) Consistent with the notion of perfect transmission, only small variations are found in $\Gamma_B^{2\text{CK}}(N_B)$ as a function of N_B (less than 0.2%), falling within our numerical precision; (iii) The Coulomb staircase in the charging of the box is completely washed out for $\Gamma_B = \Gamma_B^{2\text{CK}}(0)$, but is gradually recovered as Γ_B sufficiently departs from $\Gamma_B^{2\text{CK}}(0)$, whether above or below (inset of Fig. 2); (iv) Upon reducing E_C/Γ_L from 1 to 0.081, the ratio $\Gamma_B^{2\text{CK}}(0)/\Gamma_L$ steadily decreases from 1.72 to 1.11. This suggests the limit $\Gamma_B^{2\text{CK}} \rightarrow \Gamma_L$ as $E_C \rightarrow 0$, matching the condition for perfect transmission for two noninteracting leads. Thus, the 2CKE for $U = 0$ is well described by Eqs. (4)–(5).

So far we have considered a symmetric dot, and varied $U = -2\epsilon_d$. In reality, however, the Coulomb repulsion U

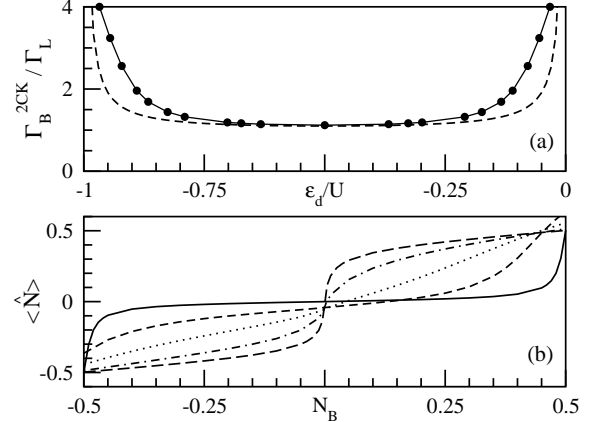


FIG. 3: (a) The two-channel line $\Gamma_B^{2\text{CK}}/\Gamma_L$ versus ϵ_d , for $U/D = 2$, $\Gamma_L = E_C = 0.1D$, and $N_B = 0$. Dashed line: The analytic estimate of Ref. [1]. (b) The charge curve $\langle \hat{N} \rangle$ versus N_B , for $\epsilon_d/D = -1, -1.581, -1.733, -1.843$, and -1.935 (solid, dashed, dotted, dot-dashed, and long-dashed line, respectively). For each value of ϵ_d , Γ_B is tuned to the corresponding $N_B = 0$ value of $\Gamma_B^{2\text{CK}}$, depicted in panel (a).

is large and fixed. The experimentally tunable parameters are the dot level ϵ_d , the dimensionless gate voltage N_B , and, to a lesser degree, the tunneling rates Γ_L and Γ_B . In Figs. 3 and 4 we explore the 2CKE as a function ϵ_d , for $U/D = 2$ and $\Gamma_L = E_C = 0.1D$. Figure 3(a) shows the two-channel line $\Gamma_B^{2\text{CK}}/\Gamma_L$ versus ϵ_d , for $N_B = 0$. The two-channel line separates two distinct Fermi-liquid states, where the dot is coupled more strongly to the box (for Γ_B above the line) or to the lead (below and to the side of the line). For comparison, the estimate of Ref. [1] for $\Gamma_B^{2\text{CK}}/\Gamma_L$ is plotted by the dashed line. There is good agreement deep in the local-moment regime, but large deviations as one approaches the mixed-valent regime.

Fixing Γ_B at the $N_B = 0$ value of $\Gamma_B^{2\text{CK}}$, the shape of the charge step dramatically changes upon going from the local-moment to the mixed-valent regime, see Fig. 3(b). For $\epsilon_d = -U/2$, one recovers a conventional Coulomb-blockade staircase, with charge plateaus at integer units of charge. Upon decreasing ϵ_d , the Coulomb staircase is gradually smeared, until it is essentially washed out for $\epsilon_d/D \approx -1.73$. Upon further decreasing ϵ_d , there is a reentrance of the Coulomb staircase. However, the degeneracy points are shifted to integer values of N_B , and the charge plateaus occur at half-integer units of charge.

To understand this surprising shift of the Coulomb staircase, we note that it happens for $\Gamma_B^{2\text{CK}}$ several times larger than Γ_L and E_C . We therefore diagonalize first the local problem of the dot and the two box degrees of freedom directly coupled to it, before incorporating the smaller scales Γ_L and E_C . For $U \gg t_B \gg U + \epsilon_d$, the ground state of the local problem is a strong admixture of the dot and box degrees of freedom, whose respective occupancies are $3/2$ and $1/2$. Switching on E_C , the remaining box degrees of freedom not directly coupled to

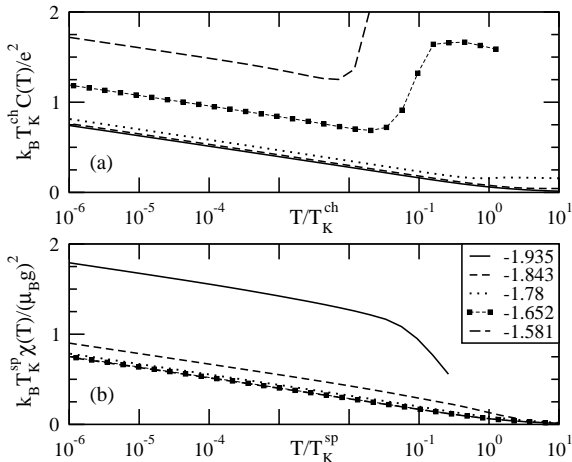


FIG. 4: (a) The capacitance of the box and (b) the magnetic susceptibility of the dot, for $U/D = 2$, $\Gamma_L = E_C = 0.1D$, $N_B = 0$, and different values of ϵ_d/D specified in the legends. For each value of ϵ_d , Γ_B is tuned to the corresponding $N_B = 0$ value of Γ_B^{2CK} . Both $\chi(T)$ and $C(T)$ diverge logarithmically as $T \rightarrow 0$, but with different Kondo scales T_K^{sp} and T_K^{ch} , extracted from the slopes of their $\log-T$ diverging terms. In going from $\epsilon_d/D = -1.581$ to $\epsilon_d/D = -1.935$, $k_B T_K^{sp}/D$ takes the values 0.0022, 0.0054, 0.0457, 0.187, and 1.72, while $k_B T_K^{ch}/D$ equals 1.035, 0.36, 0.035, 0.009, and 0.00138, respectively.

the dot thus experience an effective charging-energy interaction similar to that of Eq. (1), but with N_B shifted by half an integer. The resulting integer charge plateaus for the remaining box degrees of freedom translate then to half-integer charge plateaus for the entire box.

The most striking feature of particle-hole asymmetry is the entanglement of spin and charge degrees of freedom within the 2CKE that develops. As demonstrated in Fig. 4 for $N_B = 0$ and different values of $\epsilon_d \neq -U/2$, both the dot susceptibility $\chi(T)$ and the capacitance of the box $C(T) = (e^2/2E_C)d\langle \hat{N} \rangle/dN_B$ diverge logarithmically with $T \rightarrow 0$, when Γ_B is tuned to the corresponding $N_B = 0$ value of Γ_B^{2CK} . Quite remarkably, the degeneracy point where $C(T \rightarrow 0)$ diverges is pinned at $N_B = 0$ for all ϵ_d , even though the charge curves of Fig. 3(b) show no particular symmetry about this point. Moreover, there are two distinct Kondo scales, T_K^{sp} and T_K^{ch} , extracted from the slopes of the $\log-T$ diverging terms in $\chi(T)$ and $C(T)$. Upon decreasing ϵ_d from $-U/2$ to $-U$, T_K^{sp} monotonically increases while T_K^{ch} monotonically decreases. This marks a continuous transition from a predominantly spin 2CKE *a la* OGG deep in the local-moment regime, to a predominantly charge 2CKE *a la* Matveev in the strongly mixed-valent regime.

Experimentally, the relevant temperature scale is the crossover temperature T_0 , below which the 2CKE sets in. Estimating T_0 from the NRG level flow, we find that it roughly traces $T_{\min} = \min\{T_K^{sp}, T_K^{ch}\}$. The latter scale is greatly enhanced when the spin and charge are strongly entangled, reaching a maximum of $k_B T_{\min} \sim 0.4E_C$ for

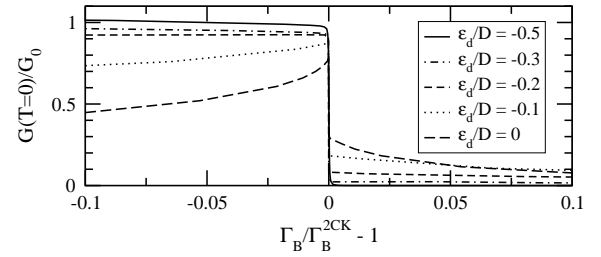


FIG. 5: The zero-temperature conductance of the two-lead device proposed by OGG [1], for $U/D = 1$, $E_C/D = 0.1$, $N_B = 0$, and different values of ϵ_d . The tunneling rates to the two leads are kept fixed, with $\Gamma_l + \Gamma_r$ equal to $0.1D$. Here $G_0/(2e^2/h)$ equals $4\Gamma_l\Gamma_r/(\Gamma_l + \Gamma_r)^2$.

the model parameters of Fig. 4. Hence, the conditions for observing the 2CKE in realistic quantum-dot devices are most favorable when the spin and charge degrees of freedom are strongly entangled.

The dot susceptibility is very useful theoretically for analyzing the 2CKE, but difficult to measure for a single dot. In Fig. 5 we depict the $T = 0$ conductance, $G(0)$, for the two-lead device proposed by OGG [1]. Here the single lead is replaced with two separate leads, characterized by the tunneling rates Γ_l and Γ_r . As noted by OGG, this setting is equivalent in equilibrium to a single lead with $\Gamma_L = \Gamma_l + \Gamma_r$. The conductance of this device is proportional at $T = 0$ to the dot spectral function at the Fermi energy, which we calculate using the NRG. Fixing Γ_l and Γ_r , $G(0)$ drops abruptly as Γ_B crosses Γ_B^{2CK} . However, in contrast to a two-channel Kondo impurity [14], the height of the conductance step is not fixed, decreasing in size with increasing charge fluctuations. Indeed, away from the Kondo limit $G(0)$ neither vanishes for $\Gamma_B > \Gamma_B^{2CK}$, nor reaches the unitary limit for $\Gamma_B > \Gamma_B^{2CK}$.

We have benefited from fruitful discussions with L. Glazman, D. Goldhaber-Gordon, Y. Oreg, D. Orgad, and R. Potok. E.L. and A.S. were supported in part by the Centers of Excellence Program of the Israel Science Foundation. F.B.A. acknowledges funding of the NIC, Forschungszentrum Jülich, under project no. HHB00.

- [1] Y. Oreg and D. Goldhaber-Gordon, Phys. Rev. Lett. **90**, 136602 (2003).
- [2] K. A. Matveev, Zh. Eksp. Teor. Fiz. **99**, 1598 (1991) [Sov. Phys. JETP **72**, 892 (1991)].
- [3] K. G. Wilson, Rev. Mod. Phys. **47**, 773 (1975).
- [4] E. Lebanon *et al.*, Phys. Rev. B **68**, 041311 (2003).
- [5] H. Schoeller and G. Schön, Phys. Rev. B **50**, 18436 (1994); J. König and H. Schoeller, Phys. Rev. Lett. **81**, 3511 (1998).
- [6] The dot susceptibility was computed by adding the Hamiltonian term $-\hat{m}H$ with $\hat{m} = (\mu_B g/2)(\hat{n}_{d\uparrow} - \hat{n}_{d\downarrow})$, and calculating the ratio $\langle \hat{m} \rangle/H$ for $\mu_B g H/D \sim 10^{-10}$.
- [7] P. D. Sacramento and P. Schlotmann, Phys. Lett. A

142, 245 (1989).

[8] A. Schiller *et al.*, Phys. Rev. Lett. **81**, 3235 (1998); C. J. Bolech and N. Andrei, *ibid.* **88**, 237206 (1998).

[9] For $U = \epsilon_d = 0$, one can first diagonalize the coupled dot and lead. This yields a model equivalent to single-mode tunneling between the box and a lead with a symmetric Lorentzian density of states of half-width Γ_L [see, e.g., E. Lebanon *et al.*, Phys. Rev. B **68**, 155301 (2003)].

[10] K. Flensberg, Phys. Rev. B **48**, 11156 (1993).

[11] K. A. Matveev, Phys. Rev. B **51**, 1743 (1995).

[12] K. Le Hur and G. Seelig, Phys. Rev. B **65**, 165338 (2002).

[13] The transformation $\psi_{R\downarrow}(x) \rightarrow -\psi_{R\downarrow}(x)$ interchanges the back-scattering and magnetic-field terms. This symmetry is violated within the expressions derived in Ref. [12].

[14] M. Pustilnik *et al.*, report no. cond-mat/0309646.